Int. J. Heat Mass Transfer. Vol. 34, No. 4/5, pp. 1149–1161, 1991
Printed in Great Britain

0017-9310/91 $3.00+0.00

Direct numerical simulation of passive heat transfer in a turbulent channel flow

S. L. LYONS and T. J. HANRATTY
Department of Chemical Engineering, University of Illinois, Urbana, IL 61801, U.S.A.

and

J. B. McLAUGHLIN
Department of Chemical Engineering, Clarkson University, Potsdam, NY 13676, U.S.A.

(*Received* 4 *January* 1990 *and in final form* 8 *June* 1990)

Abstract—A direct numerical simulation of fully developed turbulent channel flow is used to study fully developed passive heat transfer between the channel walls. The time-dependent, three-dimensional Navier–Stokes equation and the advection–diffusion equation are solved numerically with 1 064 960 grid points. No subgrid point modeling is used since all the important turbulence scales are resolved. The Reynolds number, based on the channel half-width and the bulk velocity, is 2262, and the Prandtl number is 1.

1. INTRODUCTION

UNTIL recently, numerical simulations of turbulent flow employed some form of modeling in order to simplify the governing equations. Most work prior to the present decade employed averaged transport equations for the moments of a certain order in which higher order moments were modeled. More recently, a number of investigations have employed the large eddy simulation (LES) technique in which the three-dimensional, time-dependent equations are solved but models are employed to compute the effect of subgrid-scale turbulence on the resolvable scales [1–3]. Another approach is the simple eddy modeling in which the organized, quasi-periodic structures in the viscous wall region are simulated [4–9]. However, with the advent of supercomputers, direct numerical simulations (DNS) which employ no simplifications of the governing equations for wall-bounded turbulent flows are now possible [10–17], and this paper will present the results of such a simulation for passive heat transfer in a turbulent channel flow.

In general, the dynamics of the turbulent flow field and the fluctuating temperature field are coupled. The thermal energy balance is coupled to the momentum balance through convection, and the momentum balance is coupled to the thermal energy balance through the temperature dependence of the fluid viscosity and the density. However, for small temperature differences, the influence of temperature on the physical properties of the fluid can be neglected and the momentum balance is decoupled from the thermal energy balance.

The three-dimensional, time-dependent Navier–Stokes equation and the advection–diffusion equation for the temperature field were solved in a grid of 1 064 960 points. A pseudospectral technique was used to solve the balance equations. The momentum equation was solved by using an adaptation of the Orszag–Kells approach [10]. The Orszag–Kells approach was modified to include viscous effects into the calculation of the pressure field and to ensure that continuity is satisfied at the walls [12]. The thermal energy balance was solved by a technique developed by Circelli and McLaughlin [9].

2. FORMULATION OF THE PROBLEM

The problem to be considered is that of passive heat transfer in a pressure-driven turbulent flow of an incompressible, Newtonian fluid between two infinite, flat channel walls. The bottom wall is heated and the top wall is cooled at the same rate.

The computations of the time-dependent, three-dimensional temperature and velocity fields were continued until a stationary state was reached. Two or more realizations of the spatial variation of the temperature or the velocity were then analyzed to give statistical properties. A discussion of results on the velocity field is presented elsewhere [15, 16]. Results on the temperature are given in this paper.

Of particular interest are the findings on the balances of the mean square of the temperature and of the temperature fluctuations. These are analogues of the balances of the kinetic energies of the mean flow and of the turbulence. However, a comparison must recognize differences arising from the specification of the controlling variables.

Energy for the velocity field is supplied to the flowing fluid by the pressure gradient. This energy can be directly dissipated by molecular viscosity or it can be

NOMENCLATURE

a	constant in conduction profile
H	channel half-width
i	$\sqrt{-1}$
j	integer
k_x, k_z	x- and z-components of wave vector
l	integer
L	upper limit on k_x summation
M	upper limit on k_z summation
m	integer
n	integer
N	upper limit on Chebyshev summation
N_{ke}	net production of turbulent kinetic energy
p	pressure
P	average pressure
Pr	Prandtl number
Q	generic field variable
$\tilde{Q}$	spectral transform of Q
$\mathbf{r}$	position vector
t	time or temperature fluctuation
t'	r.m.s. temperature fluctuation
T	temperature
T_n	Chebyshev polynomial of order n
ΔT	temperature difference between channel walls
u	fluctuating part of the x-component of velocity
U	mean value of the x-component of velocity
v	y-component of velocity
$\mathbf{v}$	velocity
w	z-component of velocity
x	coordinate in direction of mean flow
$\hat{x}$	unit vector in the x-direction
y	coordinate perpendicular to channel walls
$\hat{y}$	unit vector in the y-direction
z	spanwise coordinate
$\hat{z}$	unit vector in the z-direction.

Greek symbols

δ	Dirac delta function
θ	deviation of temperature from conduction profile
κ	thermal diffusivity
λ_x	periodicity length in x
λ_z	periodicity length in z
μ	dynamic viscosity
ν	kinematic viscosity
π	dynamic pressure based on fluctuating pressure
Π	dynamic pressure
ρ	density of fluid.

Subscripts

x	x-component
y	y-component
z	z-component.

Miscellaneous

∇	gradient operator
∇^2	Laplacian operator
$\bar{Q}$	average of Q over horizontal coordinates and time.

converted into turbulent velocity fluctuations. The main production of turbulence occurs close to the wall, where the velocity gradients are large, so that mean flow energy derived from the pressure gradient is convected to the wall by turbulence.

For the heat transfer problem, the source of mean-square temperature is the wall. The energy associated with the mean temperature field is carried into the fluid by conduction. It diffuses away from the wall by molecular and turbulent transport and is converted into turbulent temperature fluctuations. Because of the boundary conditions imposed on the temperature, significant gradients in the mean temperature can exist throughout the field so that production of temperature fluctuations can be important at the center of the channel as well as the wall.

A velocity field which would be more analogous to the heat transfer problem being considered is plane Couette flow for which the pressure gradient is zero and the two channel walls are moved relative to one another. Here energy is transmitted to the fluid by the work of the moving boundaries on the fluid and not by the pressure gradient.

The simulation assumes that body forces and viscous heating are negligible. The x-direction points downstream, the y-direction points in the direction perpendicular to the channel walls, and the z-direction points in the spanwise direction. The components of the fluid velocity in the x-, y-, and z-directions are denoted by $u+U$, v, and w, respectively. The computational domain is periodic in the streamwise and spanwise direction with periodicity lengths λ_x and λ_z, respectively. The distance between the channel walls is $2H$.

The momentum equation takes the form of the Navier–Stokes equation for an incompressible fluid with no body forces

$$\frac{\partial \mathbf{v}}{\partial t} + \mathbf{v} \cdot \nabla \mathbf{v} = -\nabla p/\rho + \nu \nabla^2 \mathbf{v}. \tag{1}$$

By using the identity

$$\mathbf{v}\cdot\nabla\mathbf{v} = -\mathbf{v}\times\mathbf{w}+\tfrac{1}{2}\nabla(\mathbf{v}\cdot\mathbf{v}) \tag{2}$$

where

$$\mathbf{w} = \nabla\times\mathbf{v} \tag{3}$$

the Navier–Stokes equation can be written as

$$\frac{\partial\mathbf{v}}{\partial t} = \mathbf{v}\times\mathbf{w}-\nabla\Pi/\rho+\nu\nabla^2\mathbf{v} \tag{4}$$

where

$$\Pi = p+\tfrac{1}{2}\rho\mathbf{v}\cdot\mathbf{v}. \tag{5}$$

The above form of the Navier–Stokes equation has the advantage that the convective term does not violate conservation of energy when the velocity field is expanded in a truncated Fourier–Chebyshev series [18]. The fluid is assumed to be incompressible and to satisfy rigid, no-slip boundary conditions on the channel walls

$$\nabla\cdot\mathbf{v} = 0 \tag{6}$$

$$\mathbf{v} = 0, \quad y = H, -H. \tag{7}$$

In addition, periodic boundary conditions are imposed in the downstream and spanwise directions

$$\mathbf{v}(x+m\lambda_x, y, z+n\lambda_z, t) = \mathbf{v}(x, y, z, t). \tag{8}$$

In the above equations, $\mathbf{v} = (u+U)\hat{x}+v\hat{y}+w\hat{z}$ is the velocity field ($\hat{x}$, $\hat{y}$, and $\hat{z}$ are unit vectors in the x-, y-, and z-directions, respectively), Π is the dynamic pressure, and m and n are integers.

Under steady-state conditions, a force balance shows that the external pressure gradient is given by

$$\mathrm{d}P/\mathrm{d}x = -\rho u_*^2/H \tag{9}$$

where u_* denotes the friction velocity. It is convenient to rewrite the equations of motion in dimensionless 'wall units' based on ν, ρ, and u_*. Although it is conventional to use a + superscript to denote values in wall units, the superscript will be omitted in the present paper in order to avoid cumbersome notation. From this point on, it will be understood that all quantities are expressed in wall units unless otherwise stated. The dimensionless Navier–Stokes equation takes the form

$$\frac{\partial\mathbf{v}}{\partial t} = \mathbf{v}\times\mathbf{w}-\nabla\pi+(1/H)\hat{x}+\nabla^2\mathbf{v} \tag{10}$$

where π is the dynamic pressure based on the fluctuating part of the pressure.

The thermal energy balance in an incompressible fluid with constant material properties is the advection–diffusion equation

$$\frac{\partial T}{\partial t} = -\mathbf{v}\cdot\nabla T+(1/Pr)\nabla^2 T. \tag{11}$$

In equation (11), Pr denotes the Prandtl number, which is defined by

$$Pr = \nu/\kappa \tag{12}$$

where κ denotes the thermal diffusivity. It is convenient to introduce the difference, θ, between the temperature and the temperature of a conduction profile

$$\theta = T+ay \tag{13}$$

where

$$a = \Delta T/2H. \tag{14}$$

Thus, θ satisfies homogeneous boundary conditions on the channel walls

$$\theta = 0, \quad y = -H \quad \text{or} \quad H. \tag{15}$$

It is also assumed that T and θ satisfy periodic boundary conditions in the x- and z-directions with the same periodicity lengths as $\mathbf{v}$

$$\theta(x+m\lambda_x, y, z+n\lambda_z, t) = \theta(x, y, z, t). \tag{16}$$

The initial condition for the velocity field was a parabolic velocity profile with random velocity fluctuations superimposed on it. The spanwise and streamwise velocity fluctuations were specified by a random number generator and scaled so that they were two orders of magnitude smaller than the mean velocity. The normal velocity fluctuations were determined by imposing continuity.

The initial condition for the temperature profile was the conduction profile ($\theta = 0$ or $T = -ay$). The heat transfer simulation was started after the hydrodynamic simulation had reached a steady-state so it was unnecessary to introduce random temperature fluctuations; the velocity fluctuations quickly generated a turbulent temperature field.

3. COMPUTER SIMULATION

The algorithms used to solve the governing equations are discussed in detail elsewhere [15, 17]. In this section, a brief summary of the procedures will be presented.

The Navier–Stokes equation was integrated in time using a fractional step method similar to the one discussed by Orszag and Kells [10]. The Orszag–Kells method does not include viscous effects in the evaluation of the pressure, and, as a consequence, the continuity condition is not satisfied at the channel walls. In order to avoid this problem, a Green's function method devised by Marcus [12] was used to compute the pressure field. The advection–diffusion equation was integrated in time with a fractional step method that was devised by Circelli and McLaughlin [9].

Pseudospectral methods are used to solve the Navier–Stokes equation and the advection–diffusion equation, and, for that purpose, each field variable, $Q(x, y, z, t)$, is expanded in a spectral sum

$$Q(x, y, z, t) = \sum_{k_x}\sum_{k_z}\sum_{n=0}^{N}\tilde{Q}(k_x, p, k_z)\,\mathrm{e}^{\mathrm{i}(k_x x+k_z z)}\,T_n(y/H) \tag{17}$$

where

$$k_x = \frac{2\pi}{\lambda_x} l, \quad -L \leqslant l \leqslant L-1 \tag{18}$$

$$k_z = \frac{2\pi}{\lambda_z} m, \quad -M \leqslant m \leqslant M-1. \tag{19}$$

The quantities k_x and k_z in equations (18) and (19) are the wave numbers in the x- and z-directions, respectively. The function T_n is the Chebyshev polynomial of order n. The collocation points in the y-direction are given by

$$y_j = h \cos\left(\frac{\pi j}{P}\right), \quad 0 \leqslant j \leqslant P. \tag{20}$$

When the operations are carried out directly with the field variables, $Q(x, y, z, t)$, they are said to be performed in 'physical space'. When operations are carried out with the Fourier–Chebyshev coefficients, $\tilde{Q}(k_x, p, k_z)$, they are said to be performed in 'Fourier space'. All spatial derivatives are computed in Fourier space. The computation of viscous effects and the effect of the pressure field on the velocity field are also computed in Fourier space. On the other hand, the evaluation of products such as $\mathbf{v} \times \boldsymbol{\omega}$ is performed in physical space, and this leads to aliasing errors. In principle, aliasing can be prevented by zeroing the top half of the spectrum in each direction, but this is costly in terms of the storage and time needed for fast Fourier transforms. Orszag [18] suggested that satisfactory accuracy can be obtained by applying a 'two-thirds' rule in which the top third of the spectral coefficients are zeroed. This procedure was applied to the x- and z-directions in the calculations.

The main input parameters for a simulation are the computational box lengths and the Prandtl number. The half channel height fixes the Reynolds number. The computational box size for the simulation was $H = 150$, $\lambda_x = 1900$, and $\lambda_z = 950$. The Prandtl number and the coefficient a were also set equal to unity. The only parameters that varied during the simulation were the number of grid points and the size of the time step. The heat transfer calculation was not begun until 12 500 time units after the beginning of the simulation. The size of the time step was varied during the simulation from 0.005 to 0.5; during the transient part of the simulation, a very small time step was needed in order to avoid numerical instability. The time step was kept as large as possible in order to reach a stationary state quickly. Once a stationary state was reached, the time step was reduced to 0.25. It was found that the value of the time step had little effect on the computed statistics.

The parameters L, M, and N were all equal to 64 in the calculations to be reported. Thus, the numbers of grid points along the x-, y-, and z-directions were 128, 65, and 128, respectively; the corresponding grid spacings in the x- and z-directions were 14.8 and 7.42 wall units, and the grid spacing in the y-direction varied from 0.18 wall units at the wall to 7.36 wall units in the center of the channel. It is worth pointing out that these are the spacings between the collocation points on which the non-linear terms are evaluated, but, as a consequence of the dealiasing in the x- and z-directions, the grid spacings in the x- and z-directions are three times smaller than the smallest wavelengths in those directions.

Statistical averages are functions only of y so averages were performed over x and z as well as time. The two-point correlations and the kinetic energy and thermal variance balances are based on averages over two widely spaced times, while all other averages are based on 300 time values that were taken at intervals of 2.5 wall time units. Roughly 7.5 h of CPU time on a Cray 2 computer are needed in order to simulate the channel flow over 750 wall time units. Of course, as noted earlier, one must first produce steady-state turbulence which also requires a large amount of CPU time.

4. RESULTS

The mean temperature, $\bar{T}$, and heat flux profiles across the channel are shown in Fig. 1. The heat flux is a constant across the channel showing that the temperature field is at steady state. The mean temperature has been made dimensionless with the magnitude of the wall temperature. The mean temperature profile is in reasonably good agreement with the experimental results of Page *et al.* [19] at the bottom wall and it is symmetric about the channel centerline; the reason for the asymmetry in the experimental measurements is not known. The Nusselt number predicted by the simulation is 25.36 at a Reynolds number equal to 2262, which is in excellent agreement with experimental measurements of 25.1 and 25.7 at Reynolds numbers equal to 2245 and 2340, respectively.

The intensity of the fluctuating temperature, t', is shown in Fig. 2. Also shown in Fig. 2 are the experimental measurements of Krishnamoorthy [20]; Krishnamoorthy's measurements were carried out in a turbulent boundary layer of air, and his values for the intensity have been divided by the Prandtl number of air, $Pr = 0.72$. It is interesting to note the close agreement between the numerical results and the scaled experimental values in the viscous wall region. Unlike the velocity intensities, the temperature intensity reaches a maximum at the channel centerline; this difference is due to the fact that the boundary conditions which are imposed on the temperature cause the temperature gradient to be nonzero in the center of the channel. There is a local maximum in the temperature intensity at approximately 17 wall units from the closest channel wall, which is close to the maximum in the streamwise intensity that occurs at 14 wall units. As the distance from the wall goes to zero, the intensity goes to zero linearly with a slope equal to $0.397Pr$.

The temperature–velocity correlations are shown in

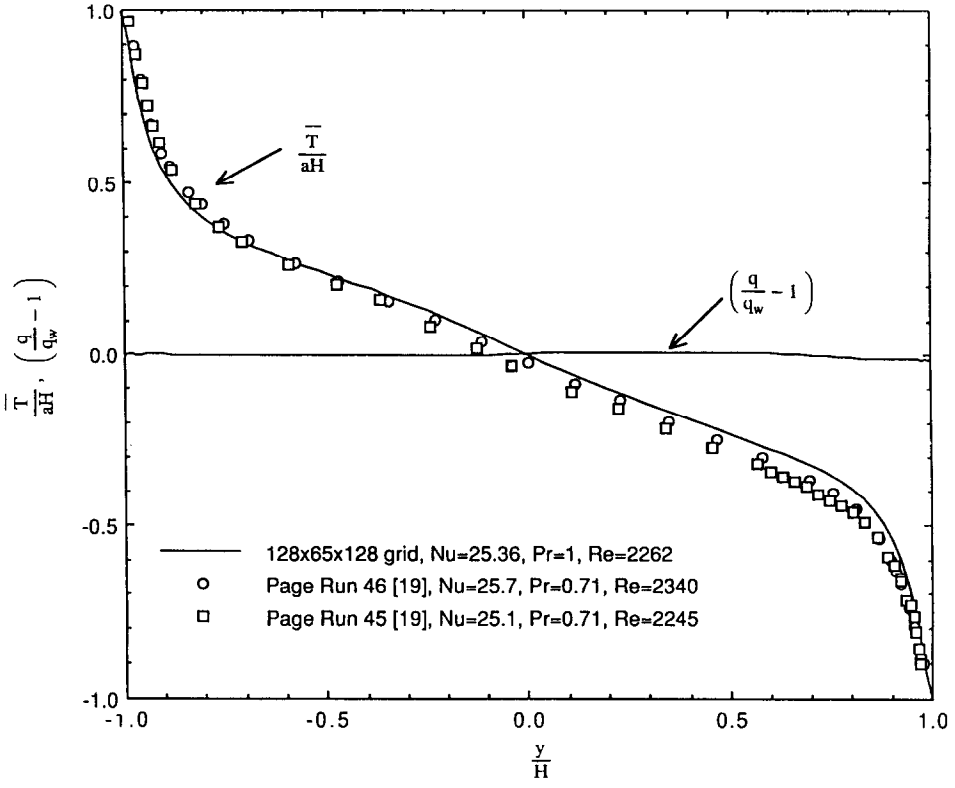

FIG. 1. Mean temperature and heat flux profiles.

Fig. 3. The bottom (hot) wall is used as the reference for $y = 0$ for the $\overline{tu}$ correlation. This correlation has the opposite sign for the top (cold) wall. As a consequence, the correlation is zero at the channel center where contributions from upward and downward fluid elements exactly cancel. The $\overline{tv}$ correlation indicates that positive temperature fluctuations correlate with positive normal velocities and that negative temperature fluctuations correlate with negative normal velocities. The $\overline{tu}$ correlation indicates that, at the bottom wall, positive temperature fluctuations correlate with negative streamwise fluctuations. Near the top wall, positive temperature fluctuations correlate with positive streamwise velocity fluctuations and negative temperature fluctuations correlate with negative normal velocities. The correlation coefficient for the streamwise velocity fluctuations is extremely large in the viscous wall region with a peak value of 0.95 at $y = 6.5$; this shows the high degree of correlation between the temperature and streamwise fluctuations in the viscous wall region.

The eddy conductivity made dimensionless with

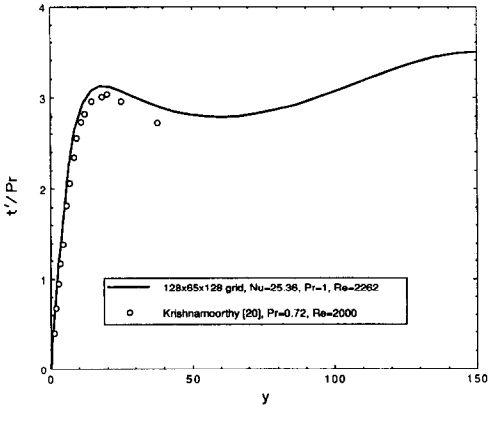

FIG. 2. Intensity of the fluctuating part of the temperature.

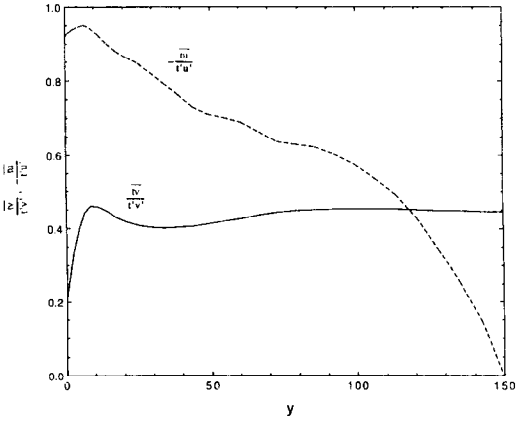

FIG. 3. Temperature–velocity correlation coefficients.

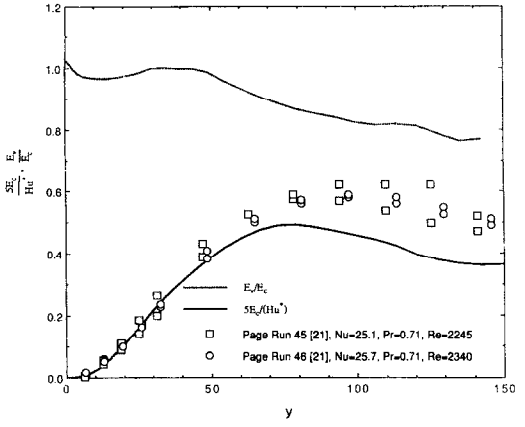

FIG. 4. Eddy conductivity and turbulent Prandtl number profiles.

mixed parameters (the channel half height and the friction velocity) is shown in Fig. 4. The profile agrees fairly well with the experimental measurements of Page *et al.* [21] in the viscous wall region, but it falls below the experimental values in the channel core. Page *et al.* computed the eddy conductivity by subtracting the contribution of molecular conduction from the total heat flux, not by measuring the temperature–normal velocity correlation. Johnk and Hanratty [22] reported that the eddy conductivity is 0.081 near the center of a pipe for the fully developed heat transfer region, and their value is in good agreement with the channel core value predicted by the simulation.

The ratio of the eddy viscosity and the eddy conductivity, the turbulent Prandtl number, is also shown in Fig. 4. The turbulent Prandtl number is close to unity throughout the viscous wall region and declines to about 0.75 near the channel centerline. This result is in agreement with the experimental results of ref. [22] which reported the turbulent Prandtl number near the center of a pipe for the fully developed heat transfer region to be 0.813, 0.769, and 0.806 at Reynolds numbers equal to 18 000, 35 000, and 71 000.

Two-point spatial correlations of fluctuating quantities are presented as a function of y and spanwise separation in Figs. 5 and 6. In both figures, the contours are for fixed values of the correlation. The contour interval is 0.05; every 5% correlation increment is shown and every 20% increment labelled. Note that the y-axis is a stretched scale. The correlations involving the temperature use the hot wall as the reference for $y = 0$.

Since the computational domain has periodicity lengths equal to 950 and 1900 in the spanwise and streamwise directions, respectively, all two-point spatial correlations with spanwise and streamwise directions must go to zero in separations equal to 475 and 950 if the periodicity lengths are large enough to resolve the largest scales of motion. It is clear from Figs. 5 and 6 that the $\overline{uu}$, $\overline{\theta\theta}$, $\overline{uv}$ and $\overline{tv}$ correlations as a function of spanwise separation are consistent with this requirement. A detailed study of other correlations as a function of both spanwise and streamwise separation confirms that the periodicity lengths were sufficiently large [16, 17].

Figure 5 presents the two-point cross-correlation with spanwise separation of the streamwise component of velocity (a) and the fluctuating part of the temperature (b). It can be seen that the correlations for the streamwise component of velocity and the temperature are almost identical. The correlations close to the wall cross zero when the spanwise separation is approximately 30 and they reach minima when the separation is approximately 52 wall units. This behavior is consistent with a streak spacing equal to 104 wall units. It is interesting to note that the correlations exhibit a second maximum at a spanwise separation approximately equal to 108 wall units, which indicates the periodic nature of the streamwise component of velocity in the viscous wall region. It should also be noted that Fig. 6(b) is consistent with Fig. 3 in that the single point cross-correlation is predicted to be approximately 0.45 in the core of the channel.

Figure 6(a) presents the two-point cross-correlation with spanwise separation of the streamwise and normal velocity components; this is the Reynolds stress correlation coefficient. The spanwise scale of motion in the viscous wall region is predicted to be approximately 100. This behavior is consistent with the periodic nature of the viscous wall region and it indicates that the spanwise scale of motion affecting the dynamics of the Reynolds stress in the viscous wall region (and, therefore, turbulence production) is 100. The correlations show that, on average, the viscous wall region is made up of alternating inflows and outflows with a wavelength equal to 100. The correlation is also strongest at $y = 12$, which is the location of the maximum turbulence production. The spanwise scale characterizing the uv product increases in the outer region to approximately 200.

Figure 6(b) presents the two-point cross-correlation with spanwise separation of the temperature and the normal velocity components. The striking similarity between Figs. 6(a) and (b) suggests that the eddy motions in the y–z plane which control momentum transport in the viscous wall region also control heat transport at the wall. On the other hand, Fig. 6(b) shows that there is a strong correlation between the temperature and the normal component of velocity, while Fig. 6(a) reveals that there is little correlation between the streamwise component of velocity and the normal component of velocity in the core of the channel. The difference between the two turbulent transport terms results from the different boundary conditions imposed on the transport equations which dictate that at the channel center the stress is zero and that the heat flux is the same as at the wall.

The budget for the variance of mean temperature is derived from equation (11)

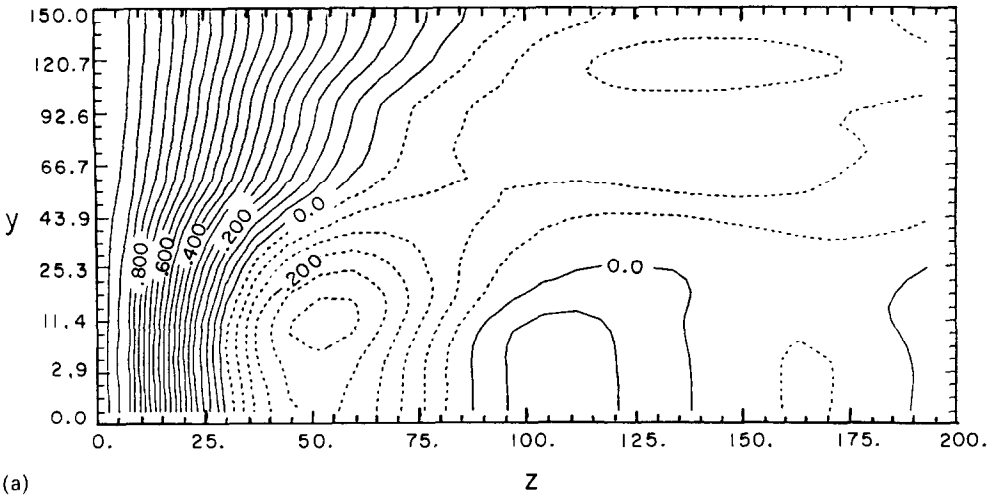

FIG. 5. (a) Two-point cross-correlation with spanwise separation for the streamwise fluctuating velocity. (b) Two-point cross-correlation with spanwise separation for the fluctuating temperature.

$$0 = \overline{tv}\frac{d\bar{T}}{dy} - \frac{d(\overline{tv}\bar{T})}{dy} + (1/Pr)\frac{d^2(\bar{T}^2/2)}{dy^2} - (1/Pr)\left(\frac{d\bar{T}}{dy}\right)^2. \quad (21)$$

The first term in equation (21) is the production of mean-square temperature fluctuations. It is a loss term that appears in the budget of the fluctuating temperature variance (see below) as a source term. The second term gives the turbulent transport of mean temperature variance. The third term is the rate of molecular diffusion of mean temperature variance. The last term gives the rate of dissipation of mean temperature variance. The terms of equation (21) are plotted in Fig. 7. In the outer flow region, $y > 50$, the turbulent transport term balances the production of temperature fluctuations. The source of mean temperature variance in the viscous wall region is the molecular diffusion term. At the wall, the rate of molecular diffusion is balanced by the dissipation rate, but the dissipation rate becomes unimportant by $y = 10$.

The budget for the variance of the fluctuating temperature is given by

$$0 = -\overline{tv}\frac{d\bar{T}}{dy} - \frac{d(\overline{t^2v}/2)}{dy} + (1/Pr)\frac{d^2(\overline{t^2}/2)}{dy^2} - (1/Pr)\left(\overline{\left(\frac{\partial t}{\partial x}\right)^2} + \overline{\left(\frac{\partial t}{\partial y}\right)^2} + \overline{\left(\frac{\partial t}{\partial z}\right)^2}\right). \quad (22)$$

The first term is the production of the turbulent fluctuating temperature. The second term is the turbulent transport of temperature fluctuations by normal velocities. The third term is the molecular diffusion of temperature fluctuations. The final term is the dissipation of temperature fluctuations. It can be seen in Fig. 8 that, throughout the channel, the two biggest

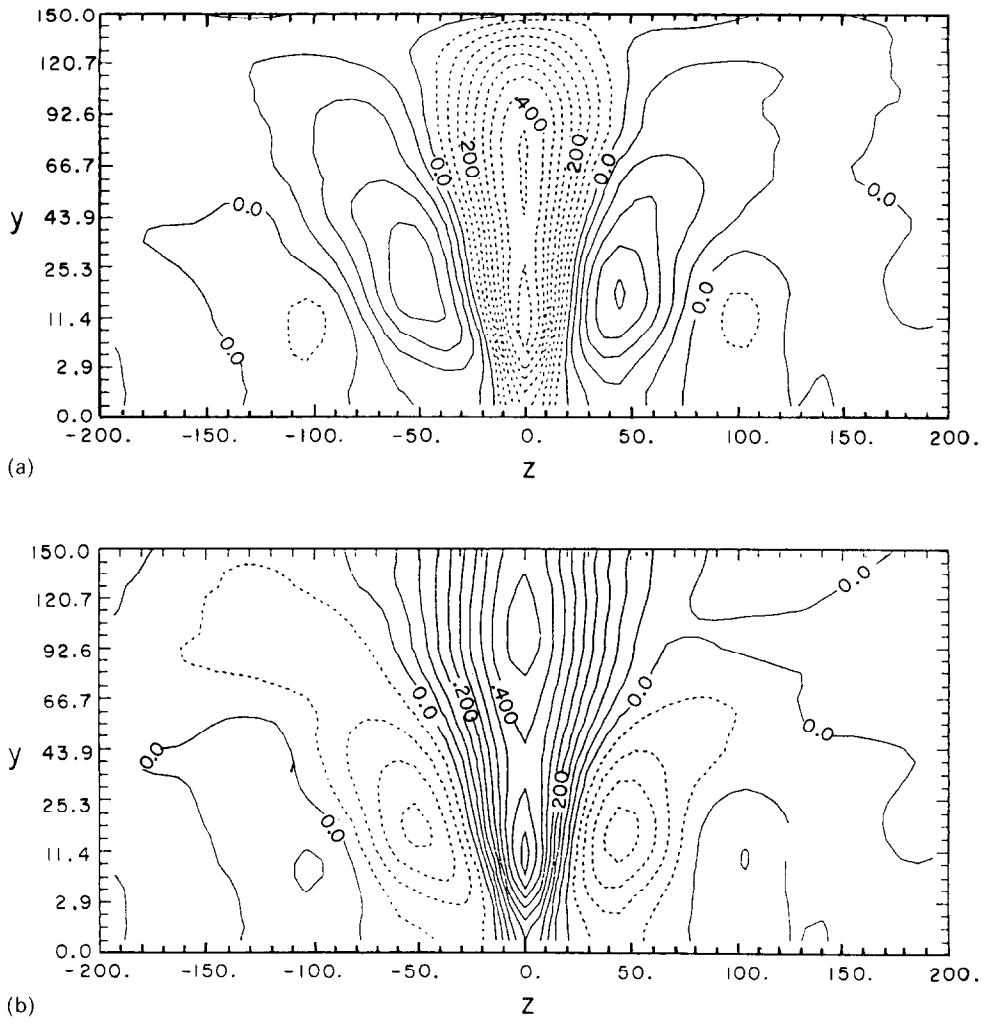

FIG. 6. (a) Two-point cross-correlation with spanwise separation for the streamwise fluctuating velocity and the normal velocity. (b) Two-point cross-correlation with spanwise separation for the fluctuating temperature and the normal velocity.

terms in the budget are the production and dissipation terms; the other two terms redistribute temperature fluctuations in the region $y < 30$. For $y > 30$, the temperature fluctuations are in equilibrium in the sense that production and dissipation are locally in balance. The profiles are qualitatively similar to those reported by Krishnamoorthy and Antonia [23] for a turbulent boundary layer. If one assumes that the numbers on the left-hand ordinate of Fig. 8 of their paper correspond to normalization with $(\delta/u_\tau\theta_\tau^2)$, where, in the notation used by Krishnamoorthy and Antonia, δ denotes the boundary layer thickness, u_τ the friction velocity, and θ_τ the friction temperature, then the results of the present paper agree well with those of Krishnamoorthy and Antonia. It should be pointed out that Krishnamoorthy and Antonia estimated the turbulent diffusion of temperature fluctuations from the closure condition rather than determining it directly from measurements.

5. DISCUSSION

The results of a direct numerical simulation of turbulent heat transfer in a fully developed turbulent channel flow are consistent with the notion that the dominant wall eddies have a spanwise scale approximately equal to 50 wall units, and that these eddies control both the production of Reynolds stress and the turbulent heat transfer. The energy balances show that the production and dissipation of thermal variance nearly balance locally throughout most of the channel.

It is instructive to contrast the terms of the balance equations for the temperature variance and the fluctuating temperature variance with the behavior of the corresponding balances for the mean kinetic energy and the turbulent kinetic energy. The transport equations for the kinetic energy and the Reynolds stress are derived directly from the Navier–Stokes equation.

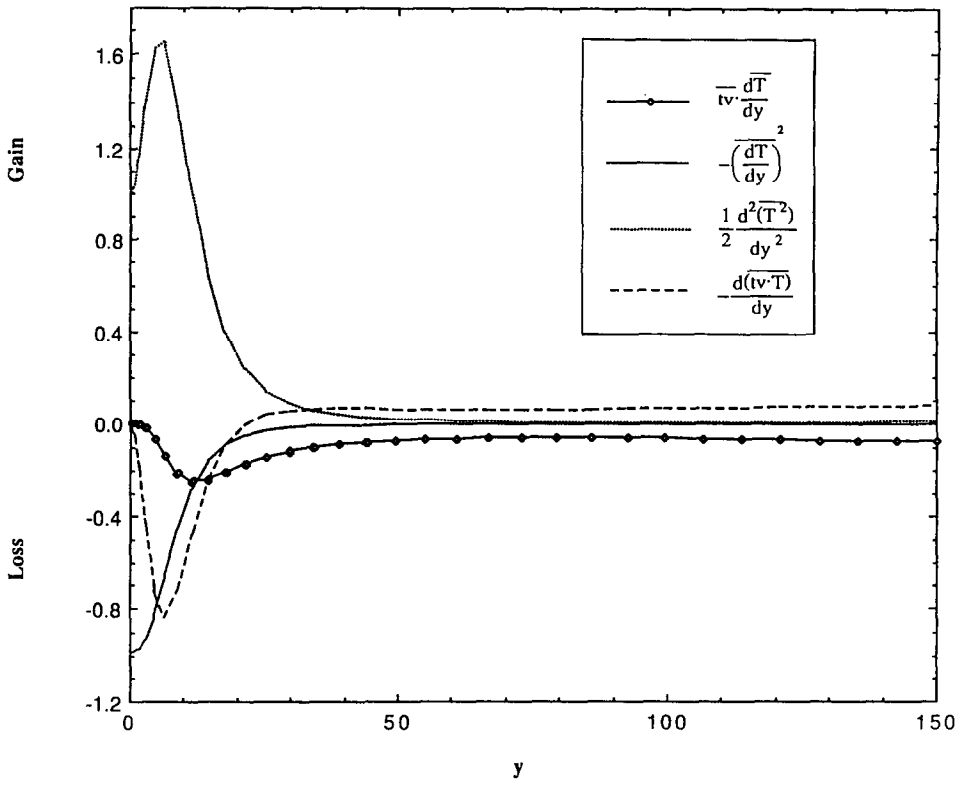

FIG. 7. Mean temperature variance budget.

The velocity and pressure are decomposed into mean and fluctuating parts, and the equations are averaged to obtain equations for the mean flow. For fully developed turbulent channel flow, the mean kinetic energy balance takes the form

$$0 = \overline{uv}\frac{dU}{dy} - U\frac{dP}{dx} - \frac{d(\overline{uv}U)}{dy} + \frac{d^2(U^2/2)}{dy^2} - \left(\frac{dU}{dy}\right)^2. \tag{23}$$

The first term in equation (23) is a loss term which appears in the turbulent kinetic energy balance (see below) as a source term giving the rate of production of turbulent kinetic energy. The second term is the mean work done by the external pressure gradient. The third term is the rate of transport of mean flow energy by turbulence. The fourth term is the rate of molecular diffusion of mean kinetic energy. The last term is the rate of dissipation of the mean kinetic energy.

The mean kinetic energy balance is shown in Fig. 9. At the wall, the rate of viscous dissipation is balanced by viscous diffusion. In the buffer region ($7 < y < 30$), all rate terms become important. The turbulent transport term and the work done by the pressure gradient balance the losses from viscous dissipation, viscous diffusion, and turbulent kinetic energy production. Outside the viscous wall region ($y > 30$), only the energy supplied by the pressure gradient is balanced by turbulent diffusion toward the wall where mean flow energy is converted to turbulence. This behavior should be contrasted with the balance for the mean temperature variance shown in Fig. 7. The source of thermal energy is at the hot wall and, therefore, in the core of the channel, the important terms are the transport of mean temperature variance and the production of turbulent temperature fluctuations.

For fully developed turbulent channel flow, the turbulent kinetic energy budget takes the form

$$0 = -\overline{uv}\frac{dU}{dy} - \frac{d\overline{q^2v}}{dy} - \frac{d\overline{pv}}{dy} + \frac{d^2(\overline{q^2}/2)}{dy^2} - \overline{\left(\frac{\partial u_i}{\partial x_j}\right)^2} \tag{24}$$

where there are implied summations over the i and j indices in the last term. The first term in equation (24) is the rate of production of turbulent kinetic energy. The second term is the rate of transport of turbulent kinetic energy by velocity fluctuations. The third term represents turbulent transport due to pressure fluctuations. The fourth term is the rate of molecular diffusion of turbulent kinetic energy. The last term is the rate of dissipation of turbulent kinetic energy.

The terms in equation (24) are shown in Fig. 10. The production of turbulent kinetic energy balances the dissipation in the region $40 < y < 100$. In the core region, $y > 100$, turbulent transport balances dis-

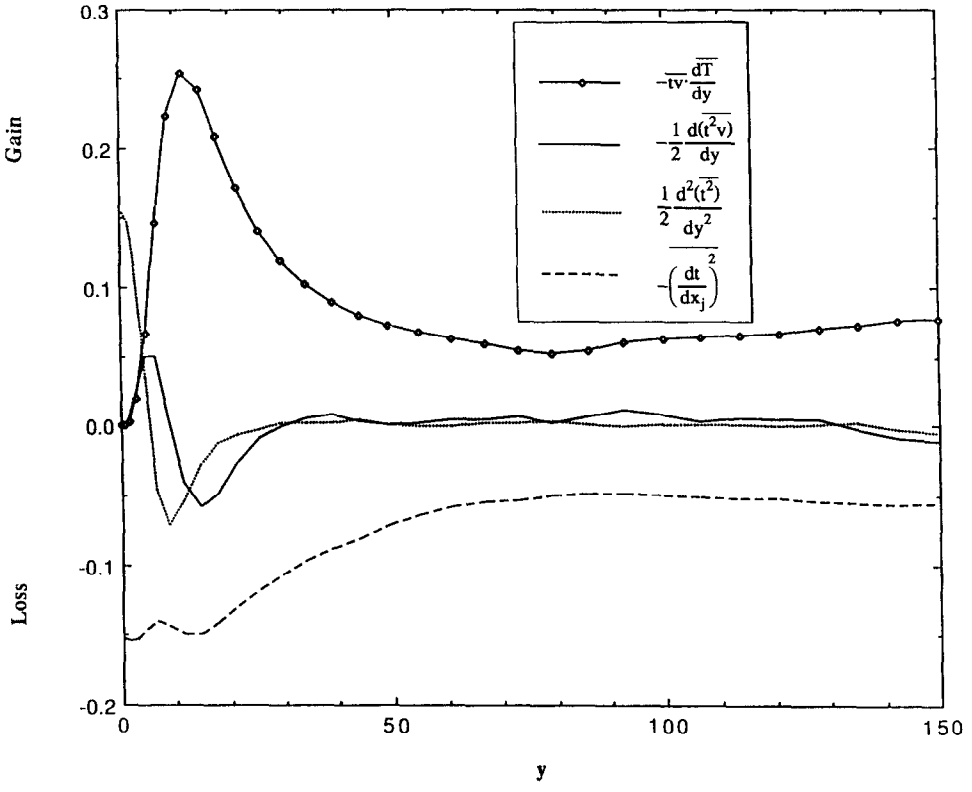

FIG. 8. Fluctuating temperature variance budget.

sipation. By contrast, Fig. 8 shows that, in the core region, the important terms in the fluctuating temperature balance are the production and dissipation of turbulent temperature fluctuations. The reason for these differences is that the mean temperature gradient is nonzero near the middle of the channel while the gradient of the mean velocity vanishes at the center of the channel.

Finally, Fig. 11 compares the net production of turbulent kinetic energy with the net production of fluctuating temperature variance. In both cases, the net production is defined by integrating the sum of local production and dissipation rates from the wall to a given value of y, where y is measured from the closest wall. For example, the net production of turbulent kinetic energy, N_{ke}, is defined by

$$N_{ke} = \int_0^y \left(-\overline{uv}\frac{dU}{dy} - \overline{\left(\frac{\partial u_i}{\partial x_j}\right)^2} \right) dy. \qquad (25)$$

Figure 11 reveals a remarkable similarity between the net production for the turbulent kinetic energy and the fluctuating temperature variance in the region $y < 40$. Near the center of the channel, the net production of thermal variance continues to rise, while the net production of the turbulent kinetic energy decreases slightly due to the fact that the gradient of the mean temperature is nonzero at the center of the channel.

6. CONCLUSION

The main results of a direct numerical simulation of passive heat transfer in a turbulent channel flow have been presented. Where possible, the computed results have been compared with published experimental results. Specifically, the mean temperature profile, the eddy conductivity profile, and the turbulent Prandtl number are in reasonably good agreement with experiment. The terms of the budget for the fluctuating variance of the fluctuating temperature are qualitatively similar to those reported by Krishnamoorthy and Antonia [23]. On the other hand, it is difficult to find detailed quantitative results for the intensity of the fluctuating temperature in the viscous wall region; previous studies have tended to focus on the logarithmic or core regions. There are no published results for the two-point cross-correlation with spanwise separation for the fluctuating temperature, the two-point cross-correlation with spanwise separation for the fluctuating temperature and the normal component of velocity, or the budget for the variance of mean temperature. In addition, Krishnamoorthy and Antonia [23] did not obtain the turbulent transport of temperature fluctuations directly from measurements.

The results reported in ref. [16] indicated that the dominant wall eddies have a spanwise scale approxi-

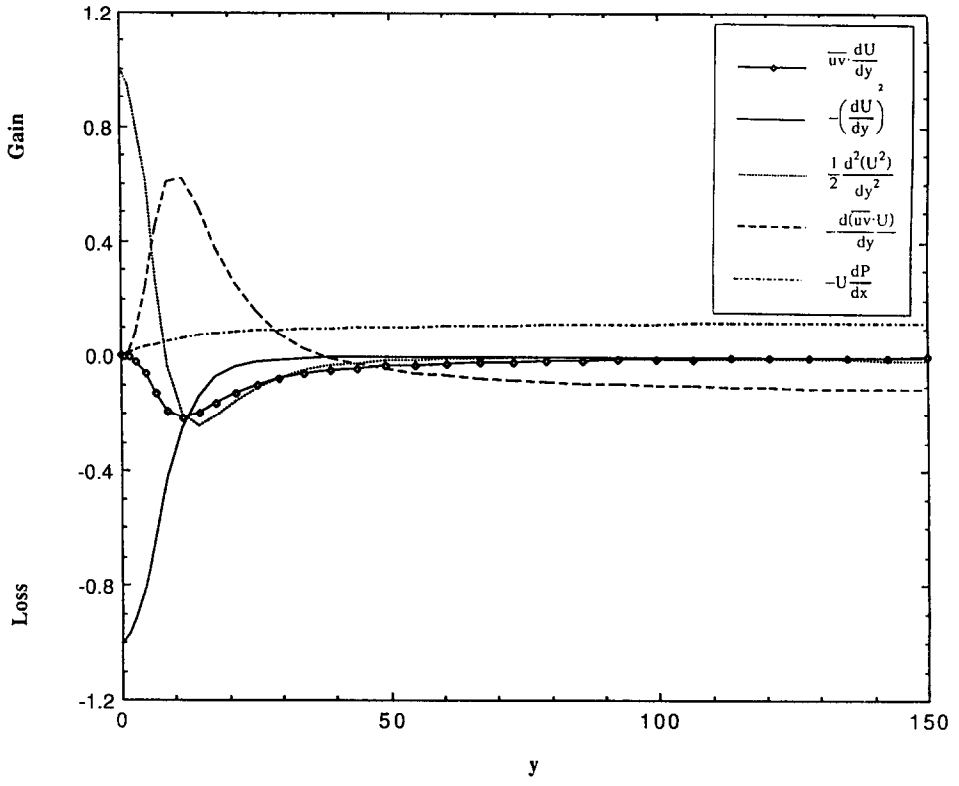

FIG. 9. Mean kinetic energy budget.

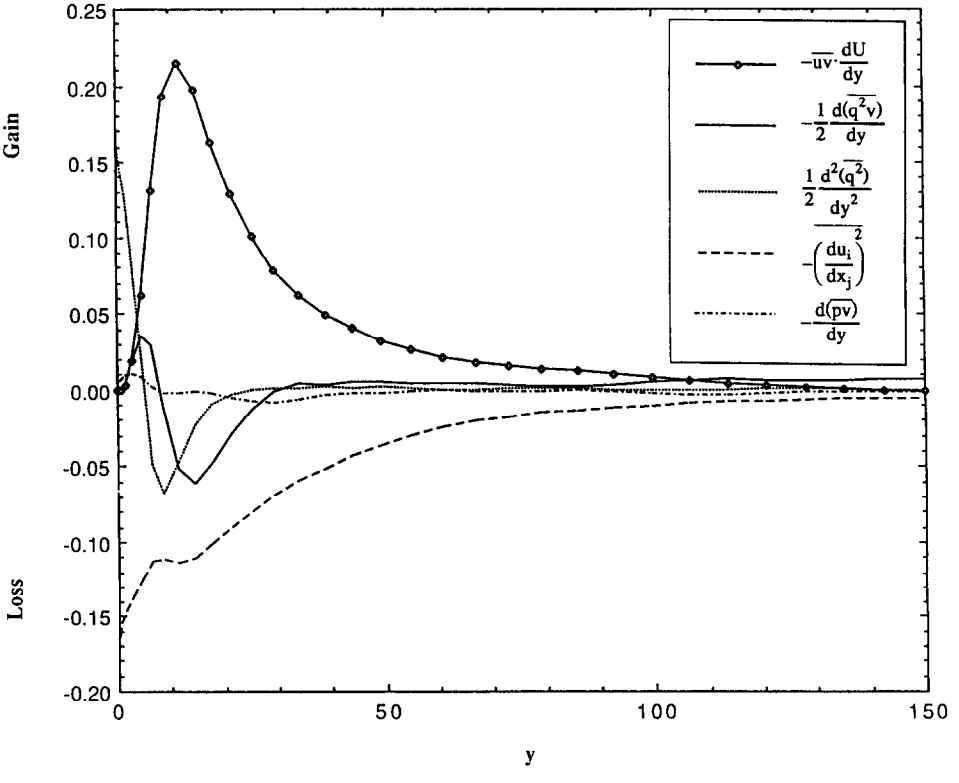

FIG. 10. Turbulent kinetic energy budget.

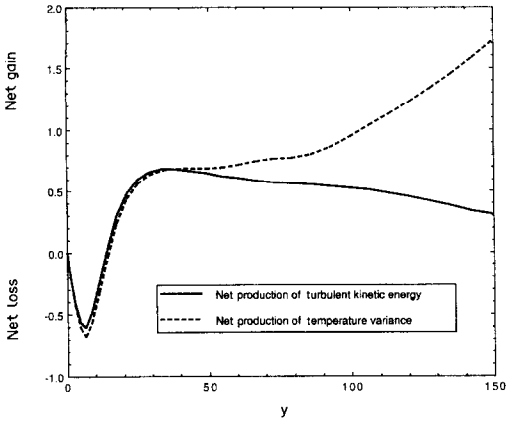

FIG. 11. Net production of fluctuating temperature variance and turbulent kinetic energy.

mately equal to 50 wall units and that these eddies control the Reynolds stress production, and, therefore, the production of turbulent kinetic energy. The two-point cross-correlations with spanwise separation in Figs. 5 and 6 of the present paper indicate that the same eddies that control Reynolds stress production also control turbulent heat transfer at the wall by transporting hot and cold fluid to and from the wall.

The fluctuating temperature budget reveals that, in the channel core, only the production and dissipation of the fluctuating temperature are significant so that the temperature fluctuations are in equilibrium. The net production of turbulent kinetic energy bears a striking similarity to the net production of fluctuating temperature variance in the region $y < 40$.

Acknowledgement—This work was supported by the Fluid Dynamics Program of the Office of Naval Research and by the Transport Phenomena Program of the National Science Foundation (T.J.H. and S.L.L.) and by the United States Department of Energy under contract DE-FG02-88ER13919 (J.B.M.). We also acknowledge the support and facilities of the National Center for Supercomputer Applications at the University of Illinois, Urbana, and at the U.S. Army Ballistic Research Laboratory at Aberdeen, Maryland.

REFERENCES

1. J. W. Deardorff, A numerical study of three-dimensional turbulent channel flow at large Reynolds numbers, *J. Fluid Mech.* **41,** 453–480 (1970).
2. U. Schumann, Ein Verhafren zur direkten numerischen Simulation turbulenter Stroemungen in Platten- und Ringspaltkanaelen und ueber seine Anwendung zur Untersuchung von Turbulenz-modellen, Ph.D. Thesis, Karlsruhe University (1973).
3. P. Moin and J. Kim, Numerical investigation of turbulent channel flow, *J. Fluid Mech.* **118,** 341–377 (1982).
4. D. T. Hatziavramidis and T. J. Hanratty, The representation of the viscous wall region by a regular eddy pattern, *J. Fluid Mech.* **95,** 655–679 (1979).
5. D. R. Chapman and G. D. Kuhn, The limiting behavior of turbulence near a wall, *J. Fluid Mech.* **170,** 265–292 (1986).
6. J. B. McLaughlin, V. Reddy and R. J. Nunge, A model of the viscous wall region of turbulent shear flows, *Chem. Engng Commun.* **41,** 181–214 (1986).
7. K. A. Azab and J. B. McLaughlin, Modeling the viscous wall region, *Physics Fluids* **30,** 2362–2373 (1987).
8. S. L. Lyons, C. Nikolaides and T. J. Hanratty, The size of turbulent eddies close to a wall, *A.I.Ch.E. Jl* **34,** 938–945 (1988).
9. B. R. Circelli and J. B. McLaughlin, A numerical study of heat transfer in turbulent shear flow, *Numer. Heat Transfer* **9,** 335–348 (1986).
10. S. A. Orszag and L. C. Kells, Transition to turbulence in plane Poiseuille and plane Couette flow, *J. Fluid Mech.* **96,** 159–205 (1980).
11. S. A. Orszag and A. T. Patera, Secondary instability of wall-bounded shear flows, *J. Fluid Mech.* **128,** 347–385 (1983).
12. P. S. Marcus, Simulation of Taylor–Couette flow, *J. Fluid Mech.* **146,** 45–65 (1984).
13. P. R. Spalart, Numerical study of sink-flow boundary layers, *J. Fluid Mech.* **172,** 307–328 (1986).
14. J. Kim, P. Moin and R. Moser, Turbulence statistics in fully developed channel flow at low Reynolds number, *J. Fluid Mech.* **177,** 133–136 (1987).
15. S. L. Lyons, T. J. Hanratty and J. B. McLaughlin, Large-scale computer simulation of fully developed turbulent channel flow with heat transfer, *Int. J. Numer. Meth. Fluids* (submitted).
16. S. L. Lyons, T. J. Hanratty and J. B. McLaughlin, Turbulence producing eddies in the viscous wall region, *A.I.Ch.E. Jl* **35,** 1962–1974 (1989).
17. S. L. Lyons, A direct numerical simulation of fully developed turbulent channel flow with passive heat transfer, Ph.D. Dissertation, University of Illinois at Urbana/Champaign (1989).
18. S. A. Orszag, Numerical simulation of incompressible flows within simple boundaries, *J. Fluid Mech.* **50,** 689–703 (1971).
19. F. Page, Jr., W. H. Corcoran, W. G. Schlinger and B. H. Sage, Temperature and velocity distributions in uniform flow between parallel plates, *Ind. Engng Chem.* **44,** 419–424 (1952).
20. L. V. Krishnamoorthy, Measurements in the near-wall region of a turbulent boundary layer, Ph.D. Dissertation, University of Newcastle (1989).
21. F. Page, Jr., W. G. Schlinger, D. K. Breaux and B. H. Sage, Point values of eddy conductivity and viscosity in uniform flow between parallel plates, *Ind. Engng Chem.* **44,** 424–430 (1952).
22. R. E. Johnk and T. J. Hanratty, Temperature profiles for turbulent flow of air in a pipe, *Chem. Engng Sci.* **17,** 867–879 (1962).
23. L. V. Krishnamoorthy and R. A. Antonia, Temperature-dissipation measurements in a turbulent boundary layer, *J. Fluid Mech.* **176,** 265–281 (1987).

SIMULATION NUMERIQUE DIRECTE DU TRANSFERT DE CHALEUR PASSIF DANS UN ECOULEMENT TURBULENT EN CANAL

Résumé—Une simulation numérique directe de l'écoulement turbulent en canal pleinement établi est utilisée pour étudier le transfert thermique passif entre les parois du canal. L'équation instationnaire tridimensionnelle de Navier–Stokes et l'équation de convection sont résolues numériquement avec une grille de 1 064 960 points. On n'utilise pas de grille plus fine parce que toutes les échelles de turbulence importantes sont résolues. Le nombre de Reynolds, basé sur la demi-largeur du canal et sur la vitesse débitante, est de 2262 et le nombre de Prandtl est égal à un.

DIREKTE NUMERISCHE SIMULATION DES PASSIVEN WÄRMEÜBERGANGS IN EINER TURBULENTEN KANALSTRÖMUNG

Zusammengassung—Die direkte numerische Simulation einer vollständig ausgebildeten turbulenten Kanalströmung wird angewandt, um den vollständig ausgebildeten passiven Wärmeübergang zwischen den Kanalwänden zu untersuchen. Die instationäre dreidimensionale Navier–Stokes-Gleichung und die Advektions-Diffusions-Gleichung wird numerisch gelöst—mit 1 064 960 Gitterpunkten. Es wird keine Modellierung in Untergittern vorgenommen, da alle wichtigen Turbulenzmaßstäbe aufgelöst werden. Die Reynolds-Zahl, die auf der halben Kanalbreite und der Kerngeschwindigkeit basiert, beträgt 2262, die Prandtl-Zahl ist gleich 1.

ПРЯМОЕ ЧИСЛЕННОЕ МОДЕЛИРОВАНИЕ ПАССИВНОГО ТЕПЛОПЕРЕНОСА ПРИ ТУРБУЛЕНТНОМ ТЕЧЕНИИ В КАНАЛЕ

Аннотация—Прямое численное моделирование полностью развитого турбулентного течения в канале используется для исследования полностью развитого пассивного теплообмена между стенками канала. Численно решаются нестационарное трехмерное уравнение Навье–Стокса и уравнение адвекции и диффузии при 1 064 960 точках сетки. Моделирование подсеточных точек не проводится, так как все важные масштабы турбулентности разрешены. Число Рейнольдса, основанное на полуширине канала и объемной скорости, составляет 2262, а число Прандтля равно 1.